Applied Surface Science 478 (2019) 319–326

Contents lists available at ScienceDirect

Applied Surface Science

journal homepage: www.elsevier.com/locate/apsusc

Full Length Article

Acid and alkali treatments for regulation of hydrophilicity/hydrophobicity of natural zeolite

Cheng Wang*, Shaozheng Leng, Huidong Guo, Liyun Cao, Jianfeng Huang*

School of Materials Science and Technology, Shaanxi Key Laboratory of Green Preparation and Functionalization for Inorganic Materials, Shaanxi University of Science and Technology, Xi'an 710021, China

ARTICLE INFO

Keywords:
Acid treatment
Alkali treatment
Natural zeolite
Hydrophilicty/hydrophobicity

ABSTRACT

Hydrophilicity/hydrophobicity property of zeolite has been received much attention in recent years. Regulation of hydrophilicity/hydrophobicity of zeolite using relative simply process and cheap raw materials is needed to be further investigated and solved. The aim of this study is to investigate effect of acid and alkali treatments on structure, hydrophilicity/hydrophobicity of natural zeolite. The structure of the samples was characterized using ICP, XRF, XRD, laser particle size analyzer, N_2 adsorption-desorption, XPS, SEM-EDX, etc. The hydrophilicity/hydrophobicity of the samples was determined using water vapor adsorption method coupled with BET specific surface area results. The results showed that acid treatment removed 5.05–23.26 wt% of aluminum from the framework of clinoptilonite using 0.1–3 M nitric acid while alkali treatment removed 0.49–7.64 wt% of silicon from the framework of clinoptilonite using 0.05–0.8 M sodium hydroxide. Accompanied by the removal of Al and Si, the specific surface area of zeolite obviously increased and decreased, respectively. Water vapor adsorptions on the alkali and acid treated zeolites with ascending SiO_2/Al_2O_3 ratio gradually decreased which confirmed the increase of hydrophobicity and decease of hydrophilicity for the samples. This acid/alkali treatment method appears to be a simple and effective way to regulate hydrophilicity/hydrophobicity of natural zeolite.

1. Introduction

Zeolites are porous hydrous aluminosilicates. The framework of zeolite typically consists of silicon-oxygen and aluminum-oxygen tetrahedrons linked by oxygen atoms. Monovalent or divalent metal cations, typically alkali metal (Na^+, K^+ etc.) or/and alkaline earth metal cations (Mg^{2+}, Ca^{2+} etc.) normally present in the zeolite framework for balancing the excess negative charge generated by Al^{3+} in place of Si^{4+} [1]. More than 40 types of natural zeolites, e.g. clinoptilolite, mordenite, have been found in the earth, while hundreds of zeolites have been artificially synthesized. The zeolites have been widely adopted in various fields due to their outstanding properties of adsorption, catalysis, ion exchange, and molecular sieve etc. [2].

The hydrophilicity/hydrophobicity has been received increasing attention due to its highly correlation with the adsorption, catalysis, ion exchange properties of zeolite [3–5]. Zeolites can change their surface hydrophilicity/hydrophobicity property with their SiO_2/Al_2O_3 ratio while the lower (higher) ratios lead to higher (lower) degrees of hydrophilicity and ion exchange capacity [6]. The zeolites with lower SiO_2/Al_2O_3 ratio and higher hydrophilicity can be applied for softening seawater [7] and hard water [8], removal of ammonium [9] and heavy metals [10] from wastewater, etc., while the zeolites with higher SiO_2/Al_2O_3 ratio and hydrophobicity can be used for removal of volatile organic compounds in air [11] and organic hydrophobic contaminations in water [12], etc. Zeolites with high (low) SiO_2/Al_2O_3 ratio can be obtained by dealuminizing (desilicating) of a specific zeolite. The dealumination can be accomplished by steaming treatments [13] and chemical agent treatments using acid [3,4,14], $(NH_4)_2SiF_6$ [15] etc. The desilication can be accomplished by alkali treatment using sodium hydrate [16–18], organic hydroxides [16] etc.

Up to now, researches on dealumination and desilication of zeolite have been investigated and a number of papers have been published [3,4,6,13–18]. However, the related published papers mainly focus on effect of dealumination and desilication towards pore structure of zeolite. In addition, the raw materials employed for dealumination and desilication are mainly synthesized zeolites, e.g. FAU zeolite [4], HZSM-5 [13,15,16], TON zeolite [17] etc. Relative limited researches have been concerned on the dealumination and desilication of natural zeolite let alone the effect of dealumination and desilication on hydrophilicity/hydrophobicity of natural zeolite [3,14,18].

* Corresponding authors.
E-mail addresses: wangcheng@sust.edu.cn (C. Wang), huangjf@sust.edu.cn (J. Huang).

https://doi.org/10.1016/j.apsusc.2019.01.263
Received 14 October 2018; Received in revised form 13 January 2019; Accepted 28 January 2019
Available online 30 January 2019
0169-4332/

China has an abundant natural zeolite mineral resource while near 400 zeolite deposits with more than 3 billion tons of zeolite ores have been discovered. The zeolite deposit located in Weichang town, Hebei province is reported to be one of the largest deposits in China. However, only limited researches about the zeolite ores from this region were reported as compared with those from other deposits, e.g. zeolite from Jinyun region, Zhejiang province [19–21].

The purpose of this study is to develop a simple and effective way for regulation of hydrophilicity/hydrophobicity of natural zeolite. For this purpose, the natural zeolite ore from Weichang region, China was adopted as a raw material, an acid/alkali treatment process was used to dealuminize/desilicate the material and the effect of acid and alkali treatments on structure and hydrophilicity/hydrophobicity of the natural zeolite were investigated.

2. Experimental

2.1. Materials

The natural zeolite sample was supplied by Beijing Guotou Shengshi Technology Co., Ltd. and zeolite ores were located in Weichang Town, Hebei province China. The zeolite ore mainly consisted of 77.77% clinoptilolite and 22.22% alpha quartz, and the chemical composition was SiO_2 (72.89%), Al_2O_3 (12.39%), K_2O (3.656%), CaO (2.5%), Fe_2O_3 (1.08%), Na_2O (0.678%), MgO (0.638%) etc. with a SiO_2/Al_2O_3 ratio of 5.88. Hydrogen nitrate (65%) and sodium hydrate (97%) were purchased from Shanghai Aladdin Biochemical Technology Co., Ltd. Acid and alkali treatments were carried out by treating of 10.0 g of pre-dried zeolite samples (60 °C for 24 h) were treated with 100 mL of 0.1–3.0 M nitric acid solutions and 0.05–0.8 M sodium hydrate solutions, respectively. The suspensions were stirred at 60 °C for 24 h and the products were washed with deionized water for at least three times and then dried at 60 °C for 24 h. The as-prepared samples were denoted as HZ0.1, HZ0.5, HZ1.0, HZ1.5, HZ2.0, HZ3.0 for the acid treated zeolites and NZ0.05, NZ0.2, NZ0.4, NZ0.8 for the alkali treated zeolites, respectively.

2.2. Sample characterization

An Optima 7300V ICP-AES spectrometer (PerkinElmer, USA) was used to analyze contents of Si and Al in the acid and alkali extracted solutions. Chemical composition of the samples was investigated using Bruker S4 Pioneer XRF (Bruker, Germany). X-ray diffraction analysis was conducted using a Bruker AXS D8-Focus diffractometer (Bruker, Germany) with Cu Kα radiation and a graphite monochromator. The operating electric current and electric voltage was 40 mA and 40 kV, respectively. The step size and exposure time were 0.01° 2θ and 0.05 s per step, respectively. Particle size distributions analysis was performed on a Mastersizer 2000 laser particle size analyzer (Malvern Panalytical, England). Specific surface area and pore size distribution analysis was conducted on a Gemini VII2390 automated physisorption analyzer (Micromeritics Instrument Corp., USA). X-ray photoelectron spectroscopy was conducted on AXIS SUPRA (Kratos Company, England) system equipped with a Al/Mg dual anode X-ray source. The pass energies for survey spectra and high-resolution spectra were 160 eV and 20 eV, respectively, and the energy step size was 0.1 eV. The binding energies were calibrated with contaminant carbon (C1s = 284.6 eV) as a reference. Morphology of the samples was conducted on a TESCAN-Vega3 scanning electron microscope, operating at accelerating voltage of 20.0 kV and work distances of 12 mm. Energy-dispersive X-ray analysis (EDX) in the SEM was taken for the chemical analysis of the samples.

2.3. Wettability determination

About 1 g of powders on weighing dish was put in a BPS-50CL temperature humidity chamber (Shanghai Yiheng Technical Co., Ltd., China) under atmospheric conditions at 30 °C, 70% humidity. Weight changes of powders were tested after 48 h of adsorption. Water vapor adsorption for mg/g [water vapor adsorption (mg)/mass of sample (g)] was calculated according to weight change of the samples before and after water vapor adsorption.

As water vapor adsorption on solids dominantly depends on the hydrophilicity/hydrophobicity and specific surface area of the solids, water vapor adsorption per unit area [mg/m^2, water vapor adsorption (mg)/surface area of sample (m^2)] was adopted to determine hydrophilicity/hydrophobicity of the samples. It was calculated based on the water vapor adsorption per unit mass and specific surface area of the samples. The calculation formula is as follows [22]:

$$W_{mm} = W_{mg}/S, \quad (1)$$

where W_{mm} is the water vapor adsorption per unit area, mg/m^2; W_{mg} is the water vapor adsorption per unit mass, mg/g; S is specific surface area of the sample, m^2/g.

3. Results and discussions

3.1. Characterization of the samples

3.1.1. Chemical composition analysis

Amount of Si and Al extracted from the alkali treated zeolites (alkali-zeolites), acid treated zeolites (acid-zeolites) and the SiO_2/Al_2O_3 ratios of the corresponding zeolites were determined based on the contents of Si and Al presented in the extracted solutions, and the results are shown in Fig. 1. It is observed that a considerable percent of Si and Al is separately removed from the zeolite ore after alkali and acid treatments, and the removal amounts of Si and Al increase with the raise of alkali and acid concentrations, respectively. Accompanied by the increase of Si and Al in the extracted alkali and acid solutions, the corresponding SiO_2/Al_2O_3 ratio of the zeolite sample decreases and increases, respectively. It is found that 0.49–7.64 wt% of silicon (0.33–1.98 wt% of aluminum) are removed from zeolite using 0.05–0.8 M sodium hydrate and the corresponding SiO_2/Al_2O_3 ratios decrease to 5.54–5.87, and 5.1–23.3 wt% of aluminum (0.08–0.26 wt% of silicon) are removed from zeolite using 0.1-3 M nitric acid and the corresponding SiO_2/Al_2O_3 ratios increase to 6.18–7.66.

In order to further determine composition of the zeolite samples, XRF was employed to analyze the zeolite, 0.4 M sodium hydrate treated zeolite (NZ0.4) and 2 M nitric acid treated zeolite (HZ2.0), and the results are shown in Table 1. It indicates that SiO_2/Al_2O_3 ratio of the NZ0.4 decreases to 5.68 while that of the HZ2.0 increases to 8.76. The XRF values of SiO_2/Al_2O_3 ratio for the alkali and acid treated zeolites are somewhat different with the ICP results, and this is probably due to the heterogeneity of raw natural zeolite or instrumental error. However, the two results have the same trend which confirms the desilication and dealumination effects of alkali treatment and acid treatment, respectively. In addition, it is found that the Na_2O content in the NZ0.4 sample obviously increases while the CaO content in the HZ2.0 sample decreases as compared with the corresponding oxides in the zeolite sample. The increase of Na_2O is attributed to the residual reaction products of sodium hydrate with zeolite while the decrease of CaO is attributed to the dissolution of Ca from the zeolite sample on the effect of nitric acid.

3.1.2. XRD analysis

Fig. 2 shows the XRD patterns of zeolite, 0.1-3 M nitric acid treated zeolite samples and 0.05–0.8 M sodium hydrate treated zeolite samples. It is clear that XRD patterns of the acid and alkali treated zeolite samples obviously change as compared with that of the zeolite sample. For the acid-zeolite samples, the (400) and (020) peaks of clinoptilolite more or less decrease with the increase of nitric acid concentration. For the alkali-zeolite samples, the (131) peak of clinoptilolite gradually

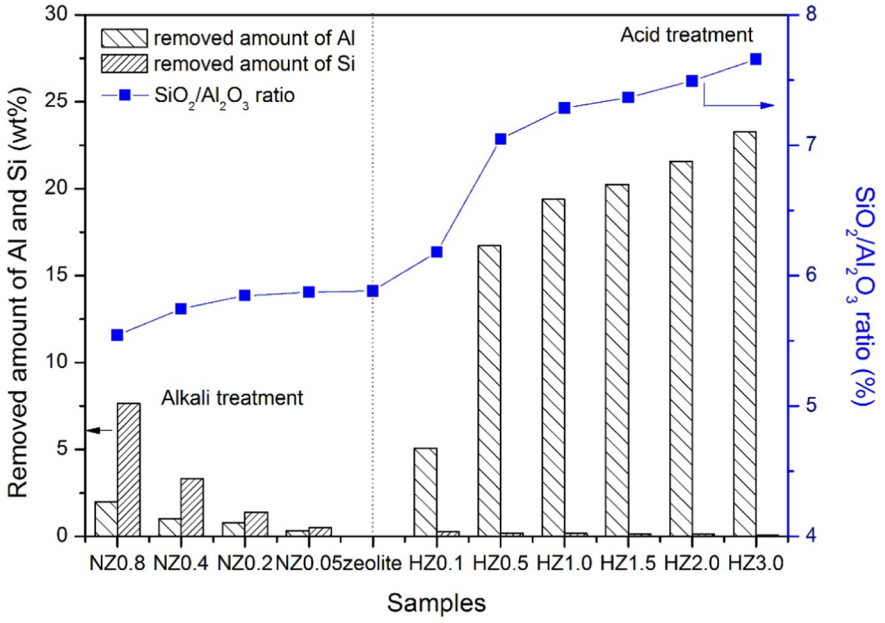

Fig. 1. Amount of Si and Al extracted from the alkali treated zeolites, acid treated zeolites and the SiO_2/Al_2O_3 ratios of the corresponding zeolites.

Table 1
Composition of zeolite, HZ0.4 and HZ2.0.

Formula/concentration (wt%)	Na_2O	MgO	Al_2O_3	SiO_2	K_2O	CaO	Fe_2O_3
Zeolite	0.678	0.638	12.39	72.89	3.656	2.5	1.08
NZ0.4	3.931	0.65	12.02	68.33	3.587	2.546	1.08
HZ2.0	0.354	0.255	9.289	81.41	3.178	0.713	0.9171

decreases with the increase of sodium hydrate concentration. These results suggest that acid and alkali treatments significantly change the structure of clinoptilolite and reduce the crystallinity of clinoptilolite. In addition, comparisons of the XRD patterns for the acid and alkali treated samples indicate that behaviors of structural change for the acid-zeolites are different with those for the alkali-zeolites, i.e. acid treatment tends to change the (400) and (020) lattice plane of clinoptilolite, and alkali treatment tends to change the (131) lattice plane of clinoptilolite. This is attributed to the removal of Al and Si from framework of clinoptilolite on the effect of acid treatment and alkali treatment, respectively. It is found that the (100) peak of quartz in alkali treated samples obviously decreases with the increase of alkali concentration while no change can be observed for the acid treated samples. This suggests that alkali treatment can change the structure and reduce the crystallinity of quartz while acid treatment has negligible effect on structure of quartz.

3.1.3. Specific surface area and pore structure analysis

Fig. 3 shows the N_2 adsorption-desorption isotherms (a) and specific surface areas, pore widths and pore volumes (b) of zeolite, acid-zeolite samples and alkali-zeolite samples. The shapes of the isotherms and hysteresis loops of the zeolite, acid-zeolites alkali-zeolites correspond to IV and H4 types, respectively (according to IUPAC), which suggests that the zeolite samples contain slit-like mesopores [23].

The specific surface area calculated from the adsorption isotherms using BET theory, average pore widths and pore volume calculated from the desorption isotherms using BJH theory of the raw zeolite sample are 27.17 m^2/g, 134.05 Å and 0.0706 cm^3/g, respectively. Specific surface areas of the acid-zeolites are obviously higher than that of the zeolite sample and the value gradually increases with the raise of acid concentration. The average pore widths obviously decrease and the

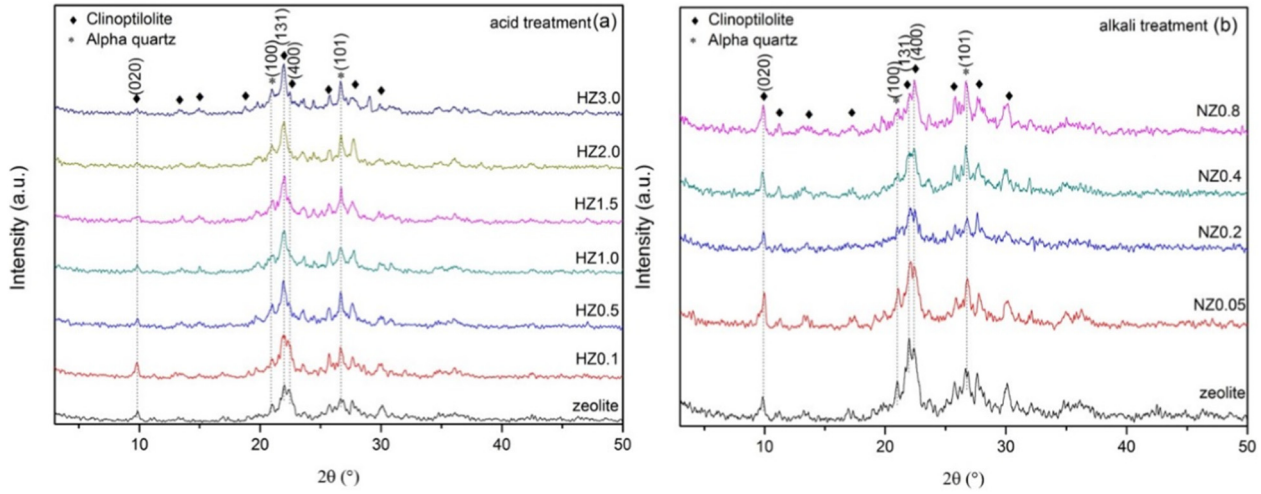

Fig. 2. XRD patterns of zeolite, 0.1–3 M nitric acid treated zeolite samples and 0.05–0.8 M sodium hydrate treated zeolite samples.

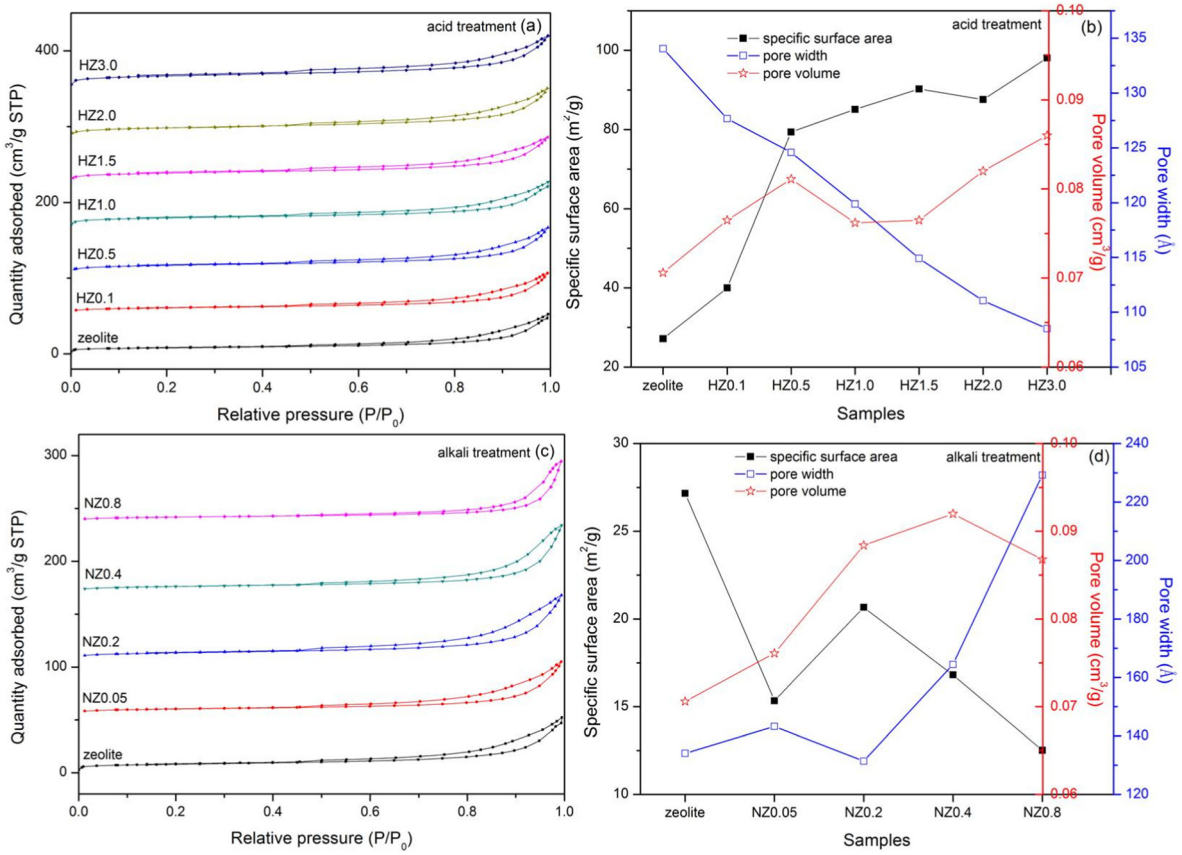

Fig. 3. N_2 adsorption-desorption isotherms (a) and specific surface areas, pore widths and pore volumes (b) of zeolite, acid-zeolite samples and alkali-zeolite samples.

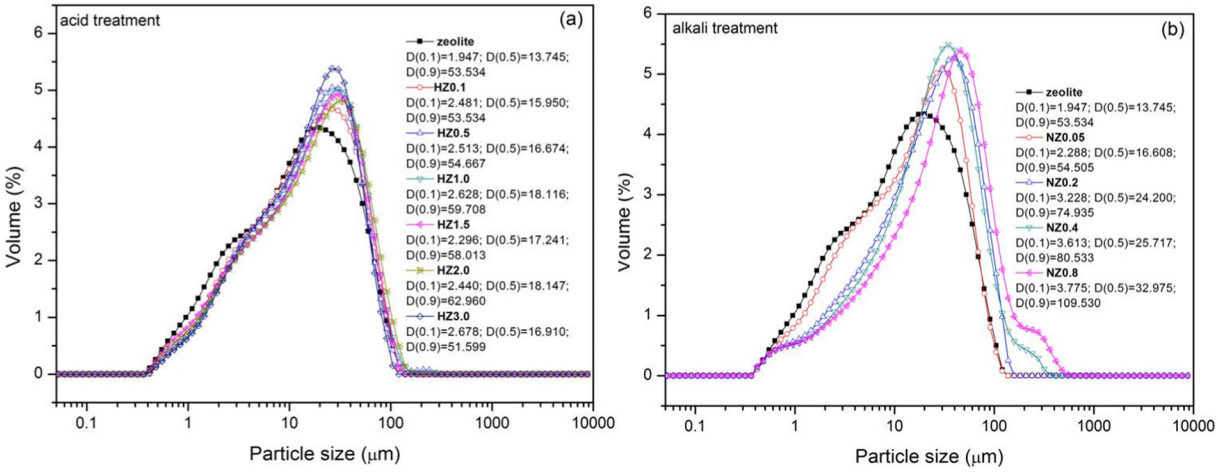

Fig. 4. Particle size distributions of zeolite, acid-zeolite samples and alkali-zeolite samples.

pore volumes slightly increase with the raise of acid concentration. However, specific surface areas and pore structures of the alkali-zeolites are different with those of the acid-zeolite. The specific surface areas of the alkali-zeolites are lower than that of the zeolite sample and the value decease with the raise of alkali concentration. The average pore widths and pore volumes gradually increase with the raise of alkali concentration. As an example, the specific surface area, pore width and pore volume of HZ2.0 are 87.59 m^2/g, 111.05 Å and 0.082 cm^3/g, respectively, while those of NZ0.8 are 12.52 m^2/g, 229.29 Å and 0.0868 cm^3/g, respectively.

The above results indicate that acid and alkali treatments can greatly change the specific surface area and pore structure of zeolite. The increase of specific surface area and pore volume and decrease of pore width for the acid-zeolites are mainly due to the dealumination of zeolite and removal of other components (e.g. calcium compounds etc.). The decrease of specific surface area, increase of pore width and pore volume for the alkali-zeolites are attributed to the desilication of zeolite and coating of sodium compounds.

3.1.4. *Particle size distribution analysis*

Fig. 4 shows the particle size distributions of zeolite, acid-zeolite samples and alkali-zeolite samples. Particle size distribution of the zeolite sample is 0.38–139 μm and the mean particle size was about 13.75 μm. Acid treatment has negligible influence on the particle size distribution of the sample with only a slight increase for the mean particle size. Particle size distribution and mean particle size of the

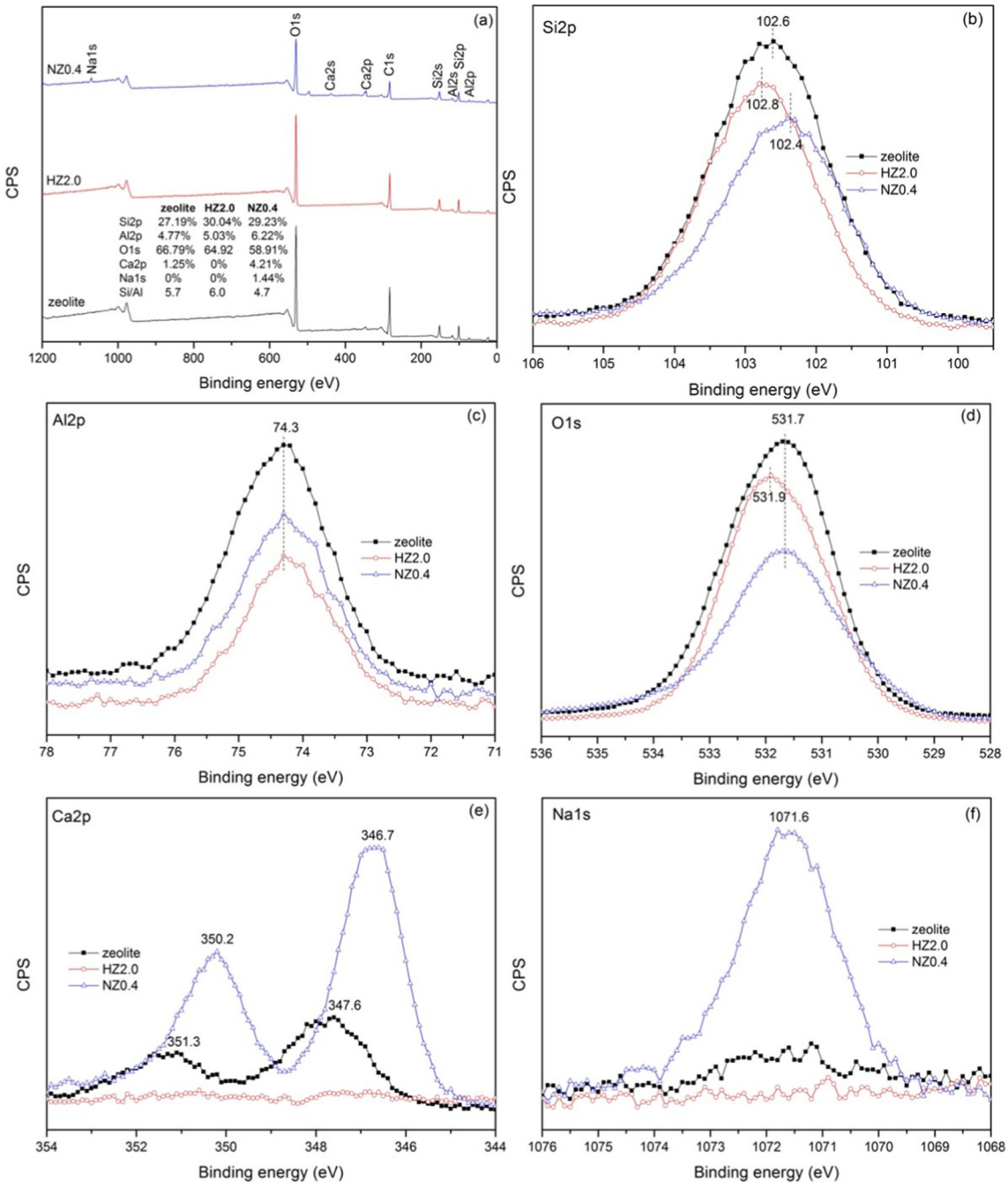

Fig. 5. XPS survey spectra (a) and XPS high-resolution spectra for Si2p (b), Al2p (c), O1s (d), Ca2p (e) and Na1s of zeolite, HZ2.0 and NZ0.4.

alkali-zeolite gradually increases with the increase of alkali concentration. As an example, the particle size distribution and mean particle size of the NZ0.8 are 0.36–540.5 μm and 32.98 μm, respectively, which are obviously bigger than those of the zeolite sample. The increase of particle size for alkali-zeolites is probably due to the aggregation of particles on the adhesion of alkali-zeolite reaction products (e.g. sodium silicate).

In purpose of further investigating the structure change of zeolite after acid and alkali treatments, the HZ2.0 and NZ0.4 were chosen and further analyzed according to their relative higher structure change based on the above analyses.

3.1.5. XPS analysis

Fig. 5a shows the XPS survey spectra of zeolite, HZ2.0 and NZ0.4. Elements of Si, Al, O, Ca and C are detected on surface of the zeolite sample and the surface Si/Al ratio is 5.7 (SiO_2/Al_2O_3 = 6.7). The surface Si/Al ratio of HZ2.0 increases to 6.0 (SiO_2/Al_2O_3 = 7.1) while that of NZ0.4 decreases to 4.7 (SiO_2/Al_2O_3 = 5.5). In addition, the Ca element has not found on the surface of HZ2.0 which is according to dissolution of Ca after acid treatment. A peak belongs to Na element appear is detected on the surface of NZ0.4 which suggests the deposition of sodium on the surface of zeolite after alkali treatment. These results are consistent with the ICP and XRF results.

XPS high-resolution spectra for Si2p, Al2p, O1s, Ca2p, Na1s in Fig. 5b–f show that Si peak for the HZ2.0 shifts to higher binding energy while that for the NZ0.4 shifts to lower binding energy. The Al2p peaks for HZ2.0 and NZ0.4 stay the same position compared with that for the zeolite sample, while their intensities obviously decrease especially for the HZ2.0 sample. The O1s peak for the HZ2.0 shifts to higher binding energy while that for the NZ0.4 stay the same position. These results

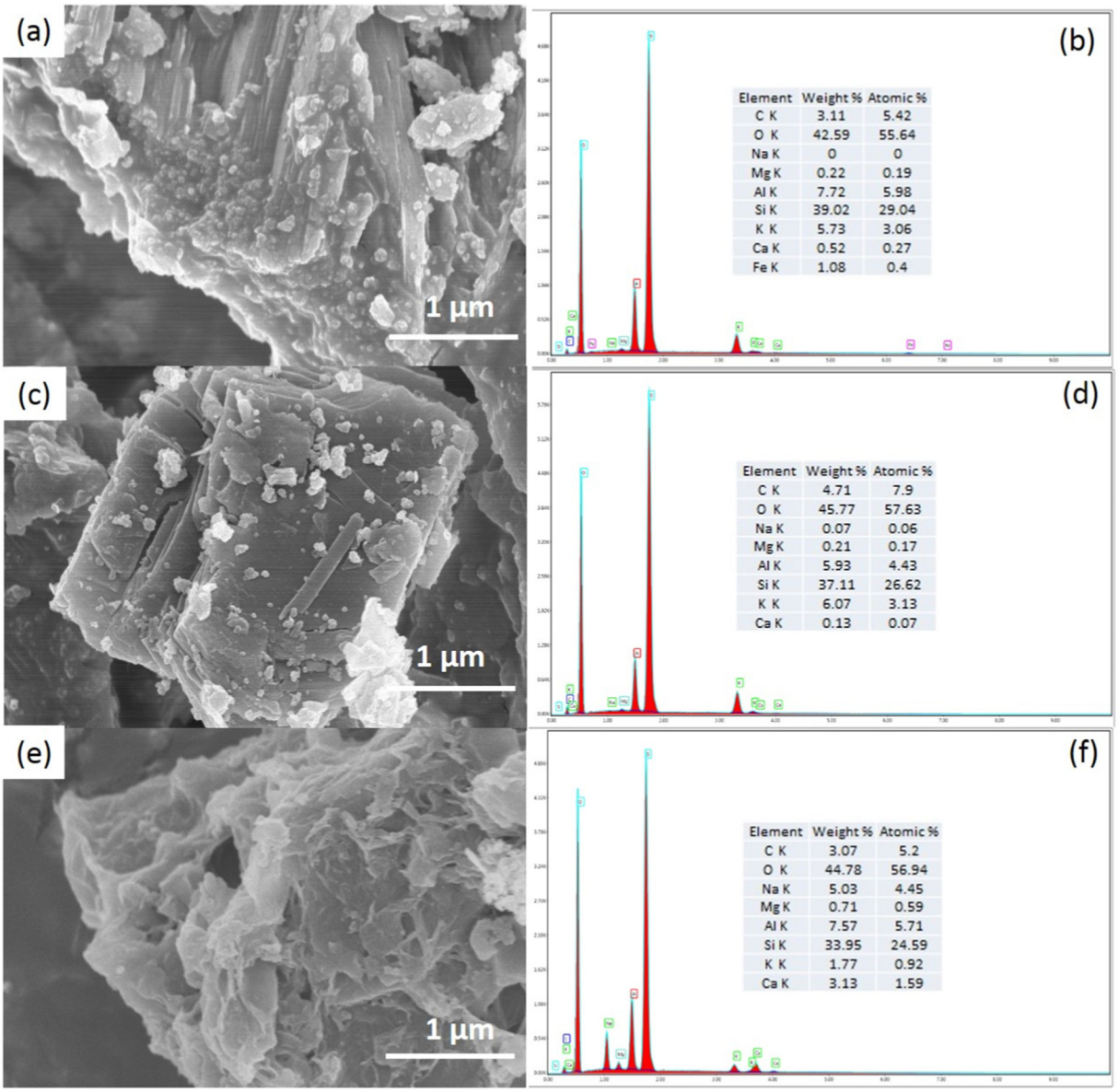

Fig. 6. SEM images and EDX spectra of zeolite (a,b), HZ2.0 (c,d) and NZ0.4 (e,f).

illustrate that removal of Al from framework of zeolite enhance covalent nature of Si—O bond within the framework while removal of Si from framework of zeolite decrease covalent nature of Si—O bond within the framework. In addition, the Ca2p peak for the HZ2.0 disappears and this further confirms the dissolution of Ca from the zeolite sample. The Ca peak for the NZ0.4 shifts to lower binding energy which suggests the decrease of ionic nature of Ca—O bond [24]. This is attributed to ion exchange of Ca ions with Na ions. The Na peak for the NZ0.4 dramatically increases as compared with the zeolite sample which is attributed to the deposition of sodium on the surface of zeolite.

3.1.6. SEM analysis

Fig. 6 shows the SEM images and EDX spectra of zeolite (a,b), HZ2.0 (c,d) and NZ0.4 (e,f). It is observed that the particles with irregular morphology are around dozens of microns while some ultrafine/nano particles also can be found on/surrounding the surface of big particles. There is no obvious difference between the zeolite and HZ2.0 which suggests that acid treatment has negligible effect on morphology of the zeolite sample. Some amount of flocculent matters appears on surface of the NZ0.4 and these flocculent matters are probably the reaction product of sodium hydrate and zeolite.

EDX results indicate that the surface chemical compositions of HZ2.0 and NZ0.4 apparently change as compared with that of the zeolite sample. Si/Al ratio of zeolite is 4.86 (SiO_2/Al_2O_3 = 5.73) while the that of HZ2.0 and NZ0.4 change to 6.0 (SiO_2/Al_2O_3 = 7.07) and 5.08 (SiO_2/Al_2O_3 = 5.08), respectively. Relative lower amount of Ca is detected on the surface of HZ2.0 while relative higher amount of Na is detected on the surface of HZ0.4. These results are consistent with the ICP, XRF and XPS results. In addition, a significant amount of K element can be found on the surface of zeolite and HZ2.0, which is consistent with the XRF result. The content of K on the surface of NZ0.4 decreases as compared with that on the surface of zeolite, and this is probably due to the ion exchange of K ions with Na ions.

3.2. Wettability of the samples

Fig. 7 shows the water vapor adsorptions per unit area on zeolite, alkali and acid treated zeolites with different SiO_2/Al_2O_3 ratio. Water vapor adsorption on the zeolite sample is 0.7362 mg/m^2 and adsorption on zeolite sample gradually increases with the decrease of SiO_2/Al_2O_3

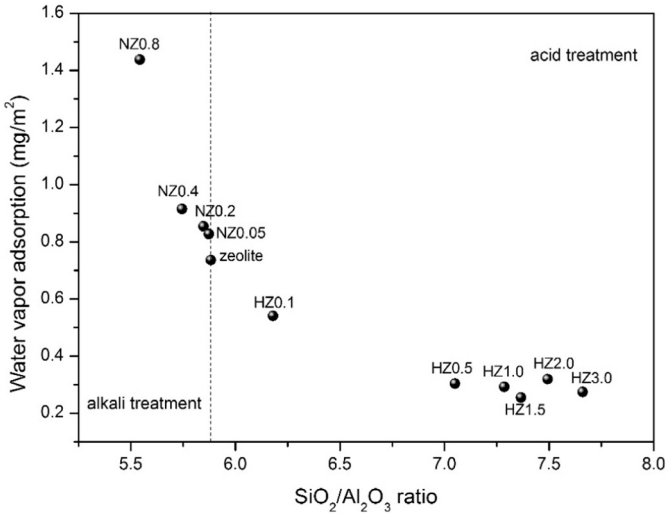

Fig. 7. Water vapor adsorptions per unit area on zeolite, alkali and acid treated zeolites with different SiO_2/Al_2O_3 ratio.

ratio. The adsorptions on 0.05–0.7 M alkali treated zeolites with SiO_2/Al_2O_3 ratios between 5.44 and 5.87 are 0.8276–1.4375 mg/m^2 while adsorption on 0.05–3.0 M acid treated zeolites with SiO_2/Al_2O_3 ratios between 6.18 and 7.66 are 0.5409–0.2747 mg/m^2.

The above results indicate that the hydrophilicity/hydrophobicity of zeolite is highly related to the SiO_2/Al_2O_3 ratio. Alkali treatment using sodium hydrate and acid treated using nitric acid is an effective way to regulate the SiO_2/Al_2O_3 ratio of natural zeolite and thus increase/decrease of the hydrophilicity/hydrophobicity of natural zeolite.

3.3. Related mechanisms

The framework of zeolite consists of SiO_4 and AlO_4 linked by O atoms. In alkaline solution, the Si—O—Si bond is easy to be attacked on the effect of OH^- and Si in the framework of zeolite can be extracted. The Si—O—Al bond is relative stable under the alkaline environment due to the negative charge of AlO_4^- which defends the Al from attack of OH^-. In acid solution, the Si—O—Al bond is unstable and Al can be easily removed from the framework of zeolite due to the opposite charged AlO_4^- and H^+. The schematic for reaction mechanisms of NaOH and HNO_3 with natural zeolite is shown in Fig. 8.

Hydrophilicity/hydrophobicity of zeolite is highly correlated with the SiO_2/Al_2O_3 ratio, and higher SiO_2/Al_2O_3 ratio means higher amount of Si—O—Si bond while lower SiO_2/Al_2O_3 ratio means higher amount of Si—O—Al bond. As Si—O—Al bond is much polar than Si—O—Si bond, higher (lower) amount of Si—O—Al bond in zeolite means that the zeolite is more hydrophilic (hydrophobic). This is the reason why the acid treated zeolites with relative higher SiO_2/Al_2O_3 ratio exhibit higher hydrophobicity and alkali treated zeolites with relative lower SiO_2/Al_2O_3 ratio exhibit higher hydrophilicity.

4. Conclusions

Sodium hydrate and nitric acid treatments were adopted in the purpose of regulation the hydrophilicity/hydrophobicity of natural zeolite from Weichang region, China. Alkali and acid treatments could effectively remove a significantly amount of Si and Al from the framework of natural zeolite and thus regulate the SiO_2/Al_2O_3 of zeolite. The removal of Si and Al on the effect of alkali and acid treatments reduced the crystallinity of clinoptilolite, and greatly changed the specific surface area and pore structure of the zeolite. The alkali and

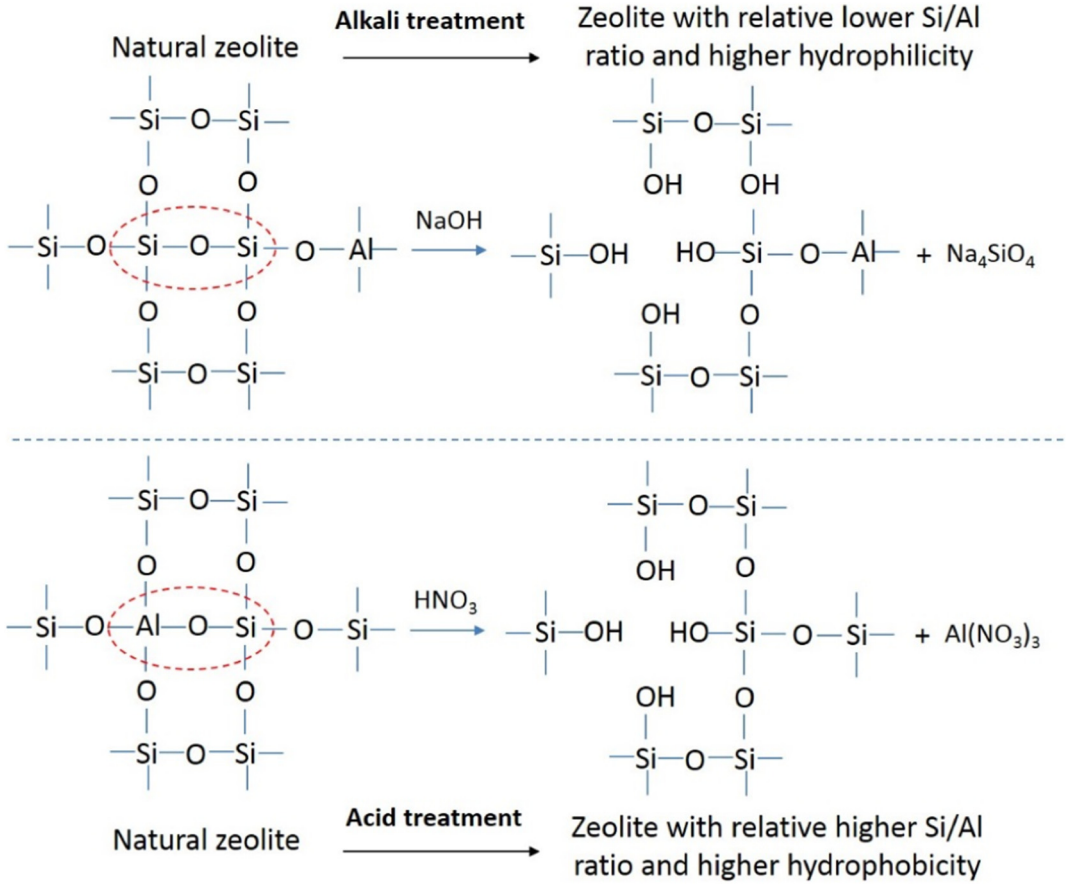

Fig. 8. Schematic for reaction mechanisms of NaOH and HNO_3 with natural zeolite.

acid treated zeolites with ascending SiO_2/Al_2O_3 ratio exhibited decreasing water vapor adsorptions per unit area and increasing hydrophobicity. This alkali and acid treatment method is a simple and effective way for regulation the hydrophilicity/hydrophobicity of natural zeolite.

Acknowledgments

The project supported by National Natural Science Foundation of China (No. 51604170), China Postdoctoral Science Foundation (No. 2016M602936XB), Shaanxi Province Natural Science Foundation of China (No. 2018JM5025), Foundation for Selected Overseas Chinese Scholar (No. 2018043) and Shaanxi Province Postdoctoral Science Foundation.

References

[1] F. Cakicioglu-Ozkan, S. Ulku, The effect of HCl treatment on water vapor adsorption characteristics of clinoptilolite rich natural zeolite, Microporous Mesoporous Mater. 77 (2005) 47–53.
[2] A. Kuleyin, Removal of phenol and 4-chlorophenol by surfactant-modified natural zeolite, J. Hazard. Mater. 144 (2007) 307–315.
[3] Y. Garcia-Basabe, I. Rodriguez-Iznaga, L.C. De, A. Lam Menorval, Step-wise dealumination of natural clinoptilolite: structural and physicochemical characterization, Microporous Mesoporous Mater. 135 (2010) 187–196.
[4] K. Yamashita, K. Kitajo, W. Shou, T. Eguchi, T. Kamegawa, K. Mori, H. Yamashita, TiO_2 photocatalyst for degradation of organic compounds in water and air supported on highly hydrophobic FAU zeolite: structural, sorptive, and photocatalytic studies, J. Catal. 285 (2012) 223–234.
[5] C. Wang, S.Z. Leng, Y. Xu, X.M. Zhang, Q.Y. Tian, L.Y. Cao, J.F. Huang, Preparation of amino functionalized hydrophobic zeolite and its adsorption properties for chromate and naphthalene, Minerals 8 (2018) 145.
[6] M. Matsui, Y. Kiyozumi, Y. Mizushina, K. Sakaguchi, F. Mizukami, Adsorption and desorption behavior of basic proteins on zeolites, Sep. Purif. Technol. 149 (2015) 103–109.
[7] T. Wajima, Ion exchange properties of Japanese natural zeolites in seawater, Anal. Sci. 29 (2013) 139–141.
[8] A.R. Loiola, J.C.R.A. Andrade, J.M. Sasaki, L.R.D. da Silva, Structural analysis of zeolite NaA synthesized by a cost-effective hydrothermal method using kaolin and its use as water softener, J. Colloid Interface Sci. 367 (2012) 34–39.
[9] R. Malekian, J. Abedi-Koupai, S.S. Eslamian, S.F. Mousavi, K.C. Abbaspour, M. Afyuni, Ion-exchange process for ammonium removal and release using natural Iranian zeolite, Appl. Clay Sci. 51 (2011) 323–329.
[10] M. Sprynskyy, B. Buszewski, A.P. Terzyk, J. Namieśnik, Study of the selection mechanism of heavy metal (Pb^{2+}, Cu^{2+}, Ni^{2+}, and Cd^{2+}) adsorption on clinoptilolite, J. Colloid Interface Sci. 304 (2006) 21–28.
[11] X.S. Zhao, Q. Ma, G.Q. Lu, VOC removal: comparison of MCM-41 with hydrophobic zeolites and activated carbon, Energy Fuel 12 (1998) 1051–1054.
[12] W.T. Tsai, H.C. Hsu, T.Y. Su, K.Y. Lin, C.M. Lin, Adsorption characteristics of bisphenol-A in aqueous solutions onto hydrophobic zeolite, J. Colloid Interface Sci. 299 (2006) 513–519.
[13] L.H. Ong, M. Dömök, R. Olindo, A.C.V. Veen, J.A. Lercher, Dealumination of HZSM-5 via steam-treatment, Microporous Mesoporous Mater. 164 (2012) 9–20.
[14] C. Wang, L.Y. Cao, J.F. Huang, Influences of acid and heat treatments on the structure and water vapor adsorption property of natural zeolite, Surf. Interface Anal. 49 (2017) 1249–1255.
[15] J.M. Müller, G.C. Mesquita, S.M. Franco, L.D. Borges, J.L. de Macedo, J.A. Dias, S.C.L. Dias, Solid-state dealumination of zeolites for use as catalysts in alcohol dehydration, Microporous Mesoporous Mater. 204 (2015) 50–57.
[16] S. Abelló, A. Bonilla, J. Pérez-Ramírez, Mesoporous ZSM-5 zeolite catalysts prepared by desilication with organic hydroxides and comparison with NaOH leaching, Appl. Catal. A Gen. 364 (2009) 191–198.
[17] P. Matias, C.S. Couto, I. Graça, J.M. Lopes, A.P. Carvalho, F.R. Ribeiro, Desilication of a ton zeolite with NaOH: influence on porosity, acidity and catalytic properties, Appl. Catal. A Gen. 399 (2011) 100–109.
[18] A. Ates, Effect of alkali-treatment on the characteristics of natural zeolites with different compositions, J. Colloid Interface Sci. 523 (2018) 266–281.
[19] D. Wen, Y.S. Ho, X. Tang, Comparative sorption kinetic studies of ammonium onto zeolite, J. Hazard. Mater. 133 (2006) 252–256.
[20] M. Huang, C. Xu, Z. Wu, Y.F. Huang, J.M. Lin, J.H. Wu, Photocatalytic discolorization of methyl orange solution by Pt modified TiO_2 loaded on natural zeolite, Dyes Pigments 77 (2008) 327–334.
[21] Y. Li, H. Li, L. Xiao, L. Zhou, T.J. Shen, X. Zhang, Hemostatic efficiency and wound healing properties of natural zeolite granules in a lethal rabbit model of complex groin injury, Materials 5 (2012) 2586–2596.
[22] C. Wang, Q. Liu, D.G. Ivey, T.H. Etsell, Bi-wetting property of oil sands fine solids determined by film flotation and water vapor adsorption, Fuel 197 (2017) 326–333.
[23] K.S. Sing, Reporting physisorption data for gas/solid systems with special reference to the determination of surface area and porosity (recommendations 1984), Pure Appl. Chem. 57 (1985) 603–619.
[24] S. Marius-Christian, C. Céline, R. Pascal, Challenges on molecular aspects of dealumination and desilication of zeolites, Microporous Mesoporous Mater. 191 (2014) 82–96.